PAPER • **OPEN ACCESS**

Numerical performance investigation of a thrust-optimized nozzle at different altitudes

To cite this article: M. G. AbuElkhier *et al* 2019 *IOP Conf. Ser.: Mater. Sci. Eng.* **610** 012071

IOP Conf. Series: Materials Science and Engineering **610** (2019) 012071 doi:10.1088/1757-899X/610/1/012071

Numerical performance investigation of a thrust-optimized nozzle at different altitudes

M. G. AbuElkhier[1,3], S. Shaaban[1] and Mahmoud Y. M. Ahmed[2]

[1]Arab Academy for Science Technology and Maritime Transport, Cairo, Egypt
[2]The Military Technical College, Cairo, Egypt

[3] E-mail: mohamedgamal202@.hotmail.com

Abstract. One of the major design aspects of jet propulsion engines is the nozzle design. The value of thrust generated by the nozzle is dependent on both the nozzle design and the flight altitude. The present paper is intended to shed more light on the jet flow structure and its evolution with flight altitude. In addition, the variation of thrust generated by the nozzle with flight altitude is addressed. A well-defined nozzle profile is adopted as a case study and numerical simulation using a commercial CFD tool is conducted. The solution method is validated by reproducing the experiments conducted on the case study nozzle.

1. Introduction

In addition to their conventional use in missiles, rocket propulsion systems nowadays find application in more civilian fields such as high-speed civil transportation and space flight. Nozzles are the devices in the rocket propulsion systems that are responsible for converting the chemical energy released upon combustion into kinetic energy. As the combustion gas products flow through the nozzle, they gain velocity on the expense of their pressure and temperature. To gain supersonic exit speeds, the well-known convergent-divergent De Laval nozzle is used. A thrust-optimized nozzle is a De Laval nozzle with a contour of the divergent section properly designed to optimize gases expansion through it thus yielding a maximum thrust. Despite its apparent simplicity, the supersonic flow downstream of De Laval nozzles incorporates a variety of interesting details. This flow problem involves shock reflections, shock-shock interactions, cap shocks, flow separations, and shock-layer interactions. The nature of flow downstream of the nozzle is dependent on many aspects including the geometry of the nozzle and the upstream (chamber, inlet) and downstream (atmospheric) pressure values.

Studying the variation of the nozzle exhaust flow pattern is essential to quantitatively assess the nozzle and the entire propulsion systems. Moreover, if thrust vectoring is sought, understanding the features of this flow is vital as far as effectiveness and structural durability of thrust vector control are concerned. The aspects of flow downstream of thrust-optimized nozzles have been studied by many researchers. For example, Pitz et al.[1] conducted an experimental investigation on a thrust-optimized nozzle at the low inlet-to-atmospheric pressure ratios that typically occur during start-up and shut-down transients. In addition, Huzel and Huang[2] developed both experimentally and computationally the cap-shock pattern at a nozzle pressure ratio of 20. Visualization of the flow pattern was conducted using hydroxyl tagging velocimetry (HTV). It was confirmed that the steady shock structures were driven by a Mach reflection with an internal shock.

In the absence of supersonic wind tunnel and advanced flow visualization facilities, such flow problem can be explored by resorting to flow simulation via CFD approach. The goal of the present study is to shed more light on the aspects of thrust-optimized nozzle exhaust flow. The objective is to conduct a numerical simulation study on the impact of the flight altitude on the features of the exhaust flow. The flight altitude is represented as the value of the atmospheric pressure. Focus is made on the variation of the flow structure and its stream-wise properties profile with the atmospheric pressure. In addition, the impact of atmospheric pressure on the thrust generated by the nozzle for the given chamber pressure is investigated. In the next section, the details of the case study and the methodology of study are illustrated. Next, the main findings are presented and discussed. The paper finalizes with the main conclusions.

2. Case study and methodology

It is desired to understand the impact of atmospheric pressure on the performance and flow structure of a thrust-optimized nozzle. The atmospheric pressure values of 1 bar, 0.75 bar, 0.5 bar, and 0.25 bar are investigated. These values of atmospheric pressure correspond to altitudes of 0, 2350, 5500, and 10300 m is standard atmosphere[3], respectively. The nozzle introduced in the experimental work[1] is used as the case study. The geometry of the nozzle is shown in figure 1, dimensions are in mm. The chamber and atmospheric pressures in the experiment were 31.3 and 1 bar, respectively.

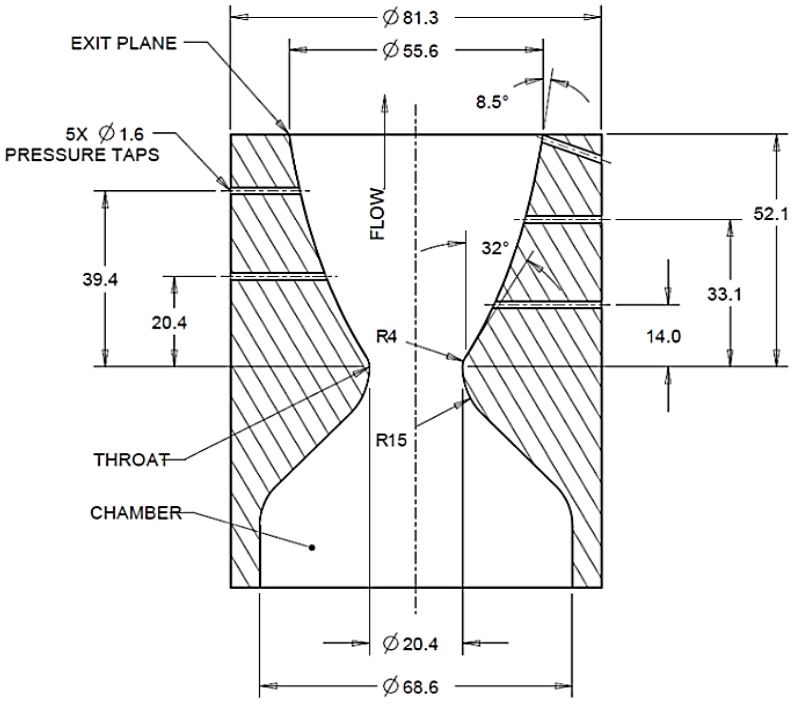

Figure 1. Dimensions of the case study nozzle[1]

The numerical simulation is conducted using the commercial finite-volume steady RANS CFD solver in ANSYS FLUENT [4] along with Spalart Allmaras turbulence model. To validate the CFD solver, the experimental work is reproduced numerically using a two-dimensional axi-symmetric computational domain. The domain is designed to incorporate the nozzle and the downstream domain. The extents and definitions of the computational domain are illustrated in figure 2, dimensions are in mm. At the pressure far field boundary, the pressure is set as the atmospheric one in the experiment. At the inlet to the nozzle, the total pressure is defined as the chamber pressure. No-slip condition is imposed at all wall boundaries.

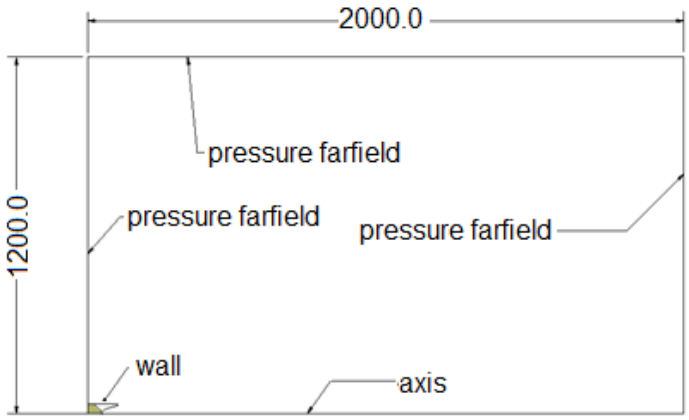

Figure 2. Computational domain and boundary conditions

The domain is discretized using a multi-block structured grid that is clustered at the walls and the parts of the domain where the key flow features are expected to take place. The discretized domain is shown in Fig.2, a zoom-in at the nozzle is shown to the right.

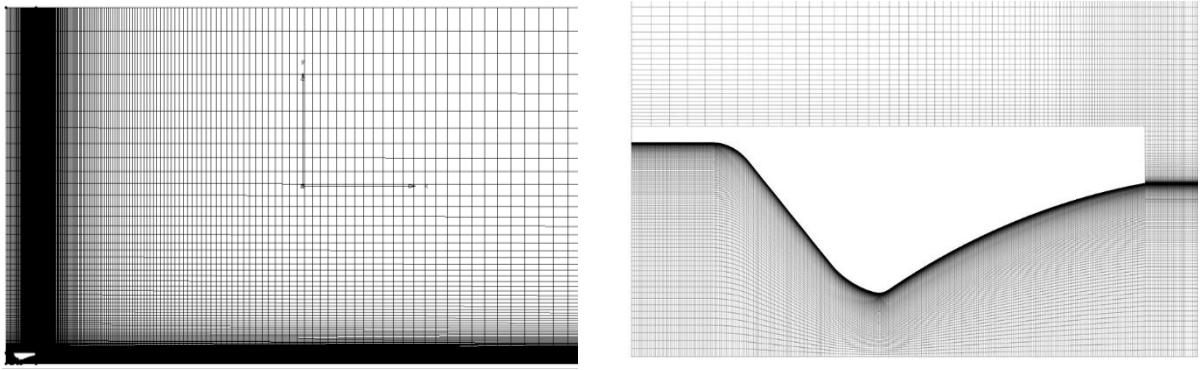

(a). The entire domain. **(b).** A zoom-in at the nozzle.

Figure 3. Structured domain

A grid sensitivity check is conducted to specify the quality of spatial resolution that yields a grid-independent solution. A fine grid is constructed (mesh0) and four coarser grids (mesh01 to mesh04) are developed by successively reducing the size by 50%. The total number of cells in the grids mesh0 to mesh04 range from 186100 to 81840, respectively. All grids are structured with first cell height of 0.001mm. To simultaneously validate the model, the experiments by Pitz et al.[1] are reproduced numerically based on the developed five grids. Figure 4 shows the results of grid sensitivity and model validation checks. The flow gage pressure along the nozzle wall is illustrated in Fig. 4a whereas flow pressure along the nozzle axis is illustrated in Fig. 4b. Clearly, a grid-independent simulation that is in a satisfactory agreement with measurements is achieved. Mesh02 grid is adopted in the following simulations.

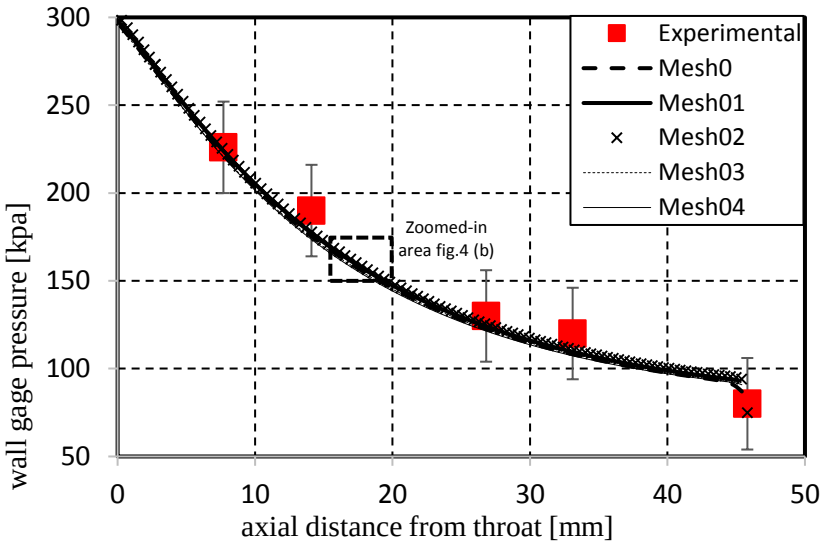

(a) Flow gage pressure profile along the nozzle wall

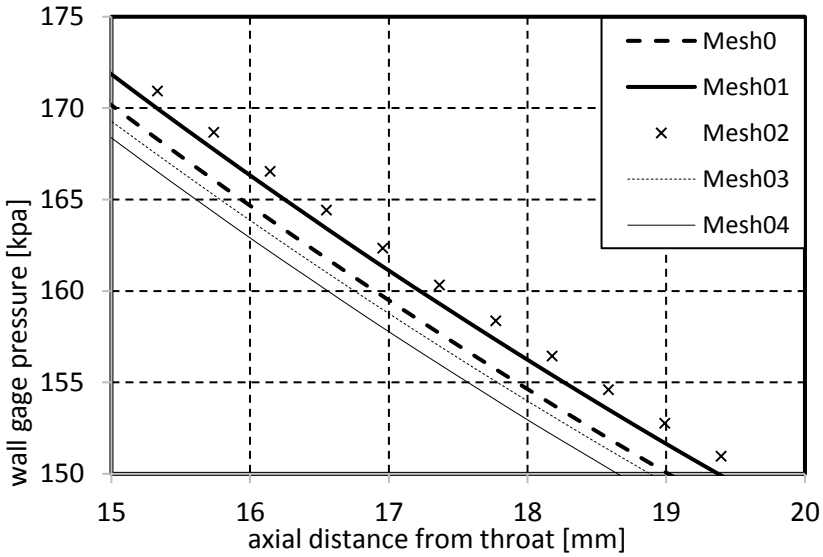

(b) A zoom-in along the nozzle wall

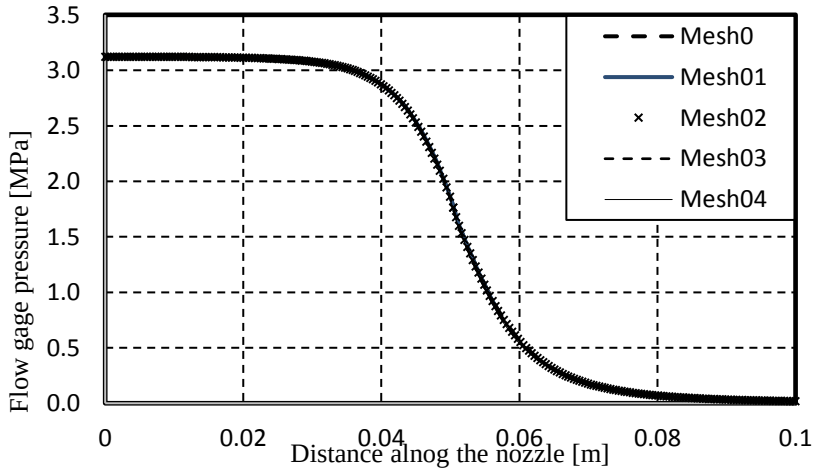

(c) flow axial gage pressure profile along the nozzle axis

Figure 4. Results of grid sensitivity and simulation model validation checks

3. Results and discussions

3.1. Variation of flow properties along the nozzle

Figure 5 below shows the variation of the flow absolute pressure and Mach number along the nozzle axis; the distance along the axis is normalized with respect to the nozzle length. Inside the chamber, the flow pressure is maximum (almost the stagnation value) and the Mach value is about 0.06. As the gases flow along the nozzle convergent section, their pressure drops and their Mach value increases sharply such that at the nozzle throat (minimum cross-section), the flow becomes sonic.

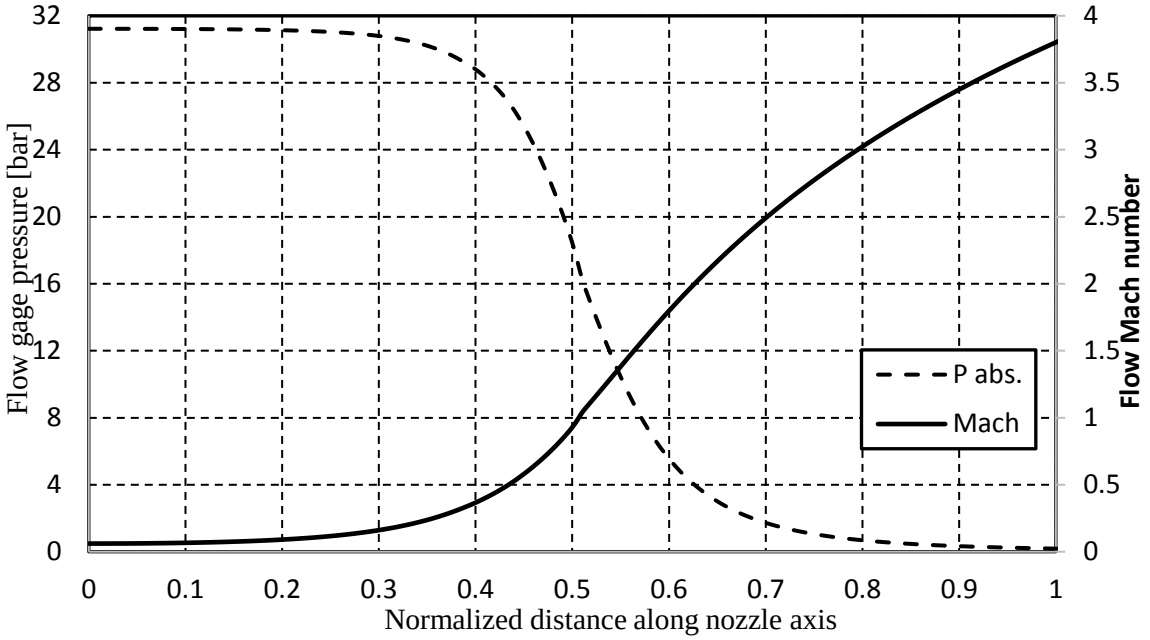

Figure 5. Variation of flow pressure and Mach number along the nozzle

Downstream of the throat, the pressure continues decreasing and Mach continues increasing with slightly lower rates. As the flow approaches the nozzle exit, its Mach number continues increasing monotonically reaching the value of 3.8. In contrast, the flow pressure comes to a near plateau trend at about 0.18 bar at the exit. This behavior of pressure is owed to the optimized profile of the nozzle divergent section which enhances the expansion profile of the flowing gases. Since they are based solely on chamber pressure and nozzle profile, the trends of pressure and Mach shown above are identical for all atmospheric pressure values examined in the numerical experiments.

3.2. Evolution of jet flow pattern with altitude

The jet flow structure at the atmospheric pressure of 1 bar is shown in Fig. 6 where the Mach contours are illustrated.

The flow expands downstream of the nozzle throat, its Mach value increases in the vicinity of the nozzle axis. In addition, following the sudden expansion downstream of the throat, the profiled contour of the divergent part causes the flow to undergo continuous compression near the walls. The combined effect is the oblique shock structure shown downstream of the nozzle followed by a large expansion wave. In addition, the boundary layer on the nozzle walls evolves to a shear layer upon exit. The shear layer engulfs the jet flow while the shock structure yields the diamond-like flow pattern that propagates downstream. The impact of freestream pressure on the jet flow structure is illustrated in the series of figure below showing the Mach contours. For comparison, the upper half of each figure shows the Mach contours for the case of 1 bar freestream pressure.

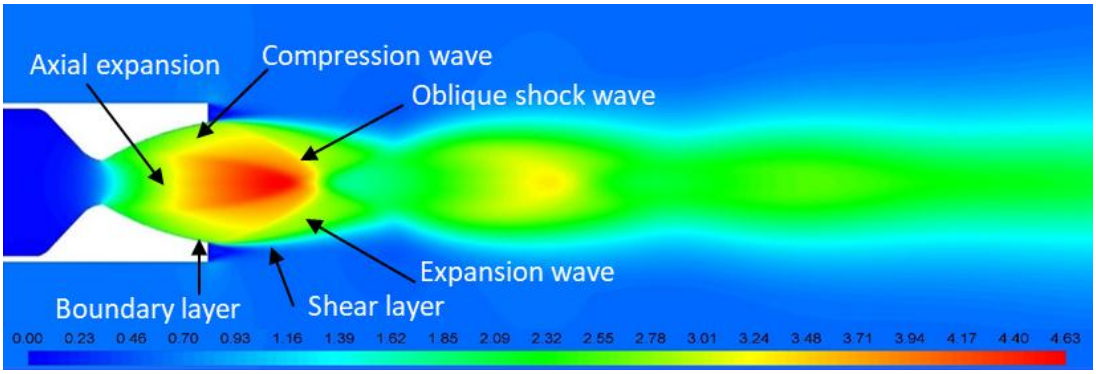

Figure 6. Jet flow structure at the atmospheric pressure of 1 bar (sea-level altitude)

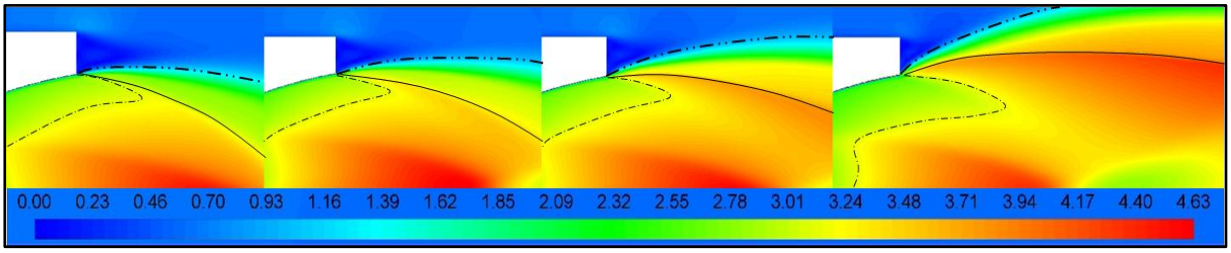

Figure 7. Schematic of the nozzle exit shock and comparison at the atmospheric pressure of 1 bar (sea-level altitude)

Generally, it can be shown that the oblique shock wave at the nozzle exit tip is further stretched outwards as the freestream pressure decreases. This causes the shock wave to be weaker and the entire jet flow pattern to get more stretched as the flight altitude increases. The evolution of flow properties downstream of the nozzle at different altitudes can be further illustrated in the figure below. Figure 8 shows the axial variation of flow pressure for different freestream pressures.

The sharp rise of pressure immediately downstream of exit (for 1 bar freestream case) indicates the location of the oblique shock wave. The subsequent sharp pressure drop is caused by the flow expansion downstream of the oblique shock. The pressure then follows the flow features until it converges to the freestream pressure at a distance of about 10 times the nozzle exit diameter. The same pattern is evident for the other values of freestream pressure. The stretching of the shock wave is addressed by the downstream shift of the pressure peak whereas the drop in this peak value reflects the drop in the shock wave strength. In all cases, the flow pressure converges to the freestream value at a long distance downstream of the nozzle.

3.3. Variation of thrust with altitude

The thrust generated by the nozzle is calculated through equation [5,6] :

$$F = \dot{m}W_e + A_e(P_e - P_a)$$

where $\dot{m}$, W_e, and P_e are, respectively, the gases flow rate, velocity and pressure as they exit the nozzle. A_e and P_a are the nozzle exit area and atmospheric pressure, respectively. The two terms on the right of the above equations represent the two thrust components referred to, respectively, as dynamic thrust and static (pressure) thrust. The variation of thrust and its components with atmospheric pressure is illustrated in Figure 9 below.

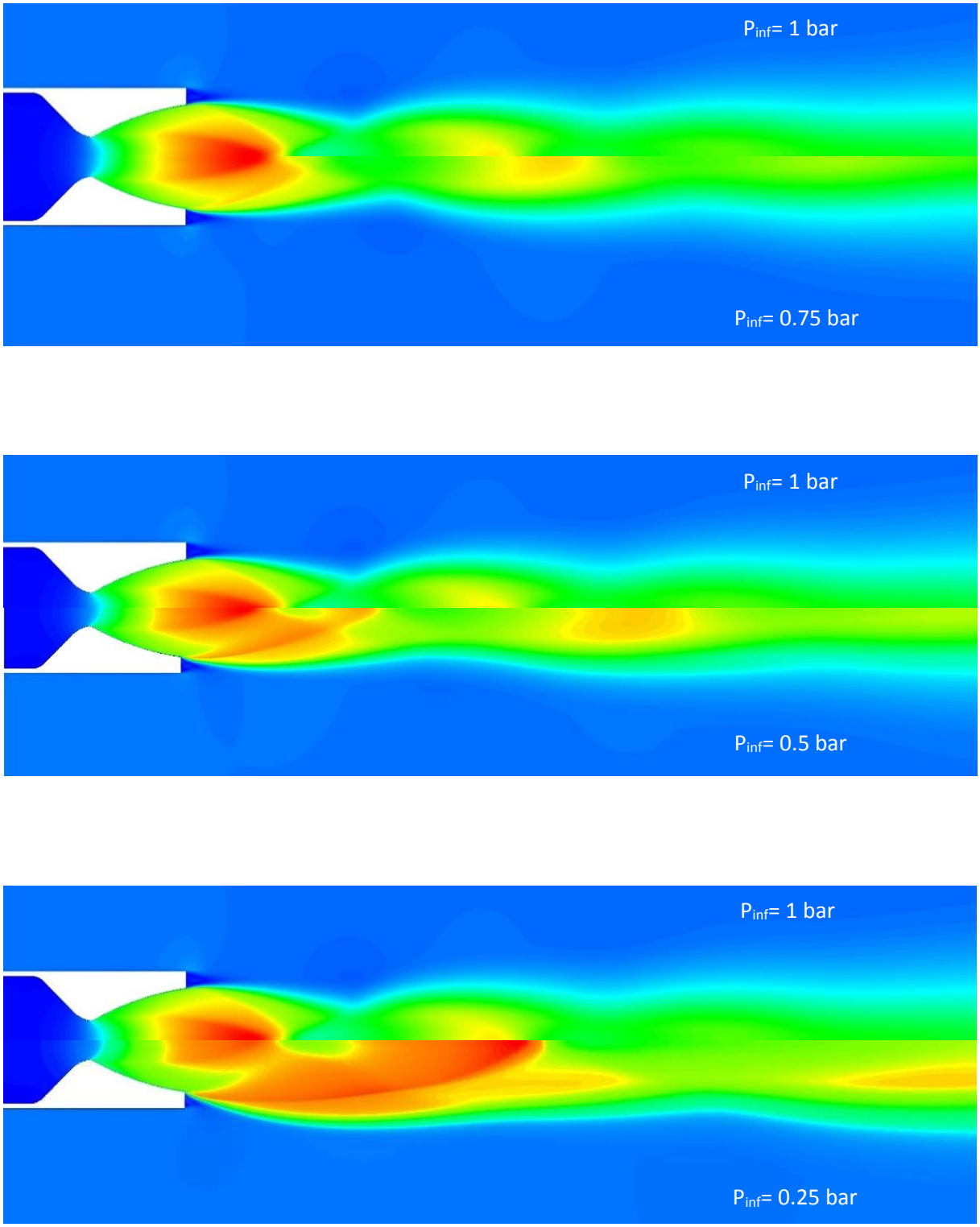

Figure 8. Impact of freestream pressure on jet flow structure

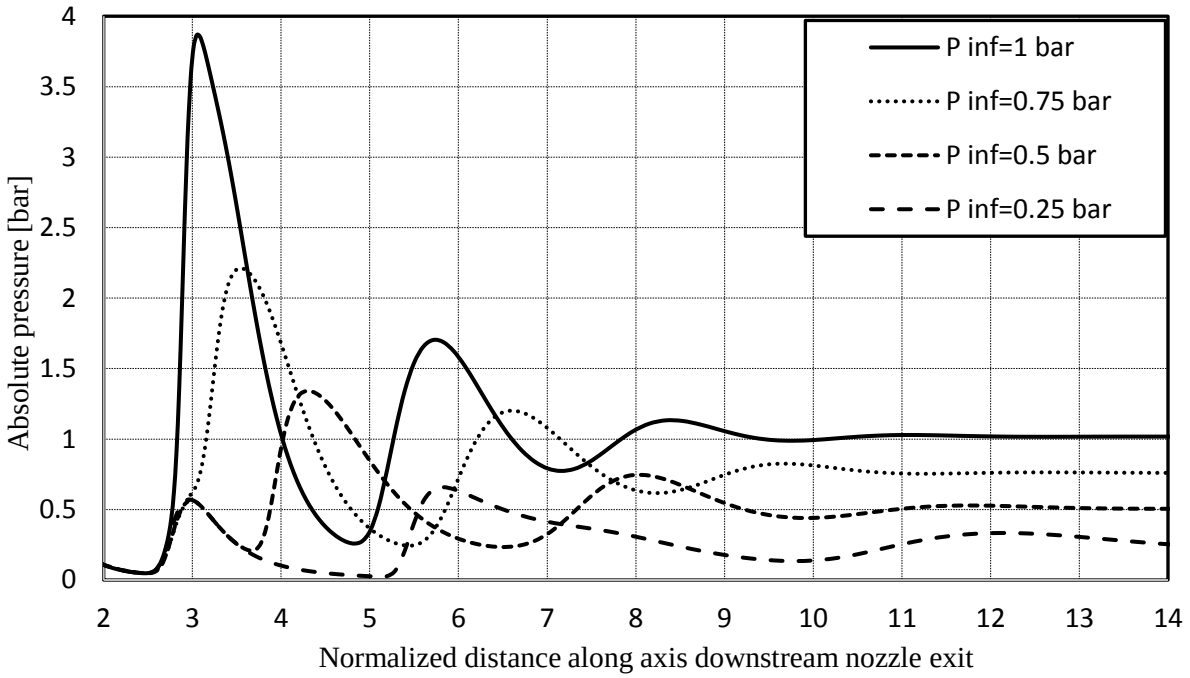

Figure 9. Impact of atmospheric pressure on the axial variation of jet flow pressure

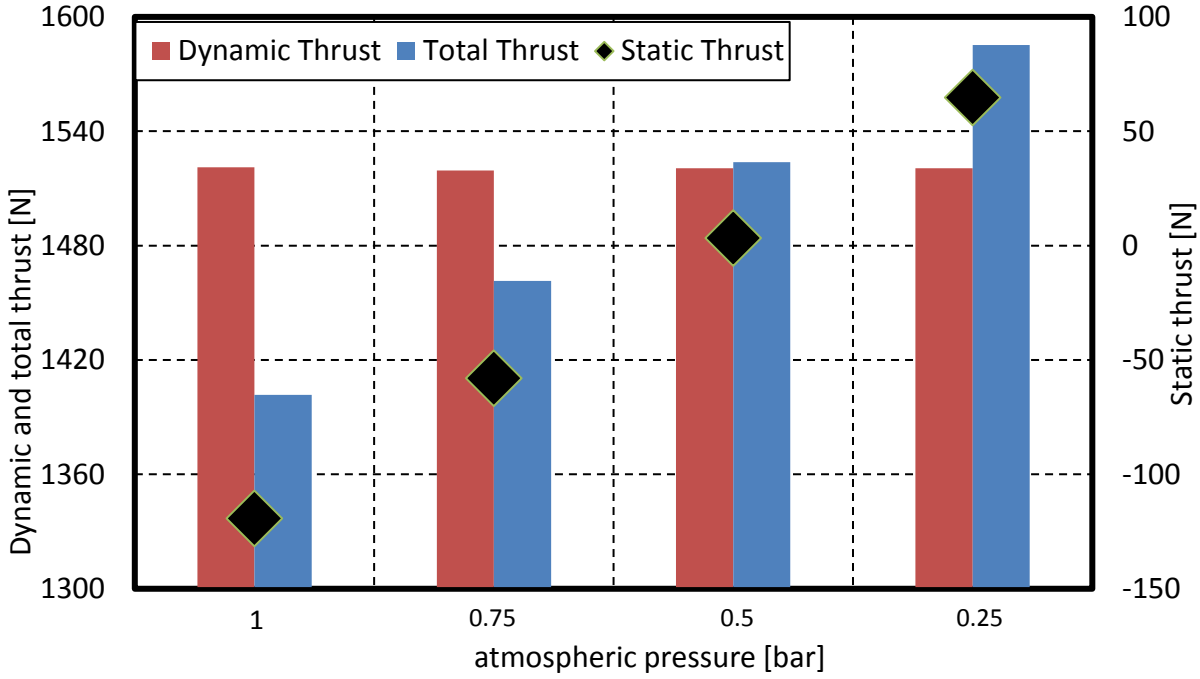

Figure 10. Impact of atmospheric pressure on nozzle thrust and its components

Clearly, the major contributor to thrust is the dynamic component due to momentum of jet flow. The value of dynamic thrust is almost independent of the atmospheric pressure. In contrast, the static thrust monotonically increases as the atmospheric pressure decreases. The static thrust can be positive or negative depending on the value of gage pressure of the flow at the nozzle exit. At the atmospheric pressure of 0.5 bar, the static thrust component nearly vanishes. This indicates that the nozzle design is adapted to the flight altitude of about 2350 m above the sea level in a standard atmosphere. For lower altitudes, the flow through the nozzle is said to be over-expanded while for higher altitudes, the flow is said to be under-expanded. Overall, the total nozzle thrust increases monotonically with the increase in altitude.

4. Conclusion

The nozzle is the key element in the rocket motor responsible for generating the thrust. The value of generated thrust, jet flow properties, and the jet flow pattern are mainly dependent on the flight altitude represented as the freestream pressure. The focus of the present study was to examine the impact of freestream altitude on the thrust and jet flow structure. A commercial CFD tool was implemented and validated by comparing with published experimental results. It was found that, the dynamic component of thrust, the major part, is almost invariable with the flight altitude. In contrast, the static component, the minor part, increases monotonically with altitude. Overall, the thrust is found to monotonically drop with lower altitude. Finally, the evolution of jet flow pattern with altitude was investigated.

References

[1] R. Pitz, M. Ramsey, W. Anderson, T. Jenkins, Y. Matsutomi, and C. Yoon, “Experimental Velocity Profiles in the Cap Shock Pattern of a Thrust Optimized Rocket Nozzle,” 49th AIAA Aerosp. Sci. Meet. Incl. New Horizons Forum Aerosp. Expo., no. January, pp. 1–12, 2011.
[2] D. H. Huzel, and D. K. Huang, Design of Liquid Propellant Rocket Engines. 1971.
[3] NASA-TM-X-74335, U. S. Standard Atmosphere, October, 1976.
[4] ANSYS FLUENT 14.5 user’s guide., ANSYS Inc.
[5] Barrerre, M., Rocket Propulsion, Elsevier, New York, 1960.
[6] Sutton, G., and Biblarz, O., Rocket Propulsion Elements, 8th ed.,Wiley, Hoboken, NJ, 2010.